Diyala Journal of Engineering Sciences

ISSN 1999-8716
Printed in Iraq

Vol. 04, No. 01, pp. 12-29, June 2011

ELASTIC- PLASTIC ANALYSIS FOR SQUARE SHELL TUBES DURING PURE BENDING USING FINITE ELEMENT

Eklas Edan Kader
Engineering Collage, Diyala University
(Received:12/4/2010 ; Accepted:5/1/2011)

ABSTRACT :- An analytical model with sufficiently non linear kinematics to capture the development in engineering applications to resist bending stress for thin walled elastic-plastic steel tubes which used as structural members. The results indicate that collapse of such tubes is imperfection sensitive for tubes with height to thickness ratio (h/t), but the sensitivity decreases as the ratio decreases. Experimentally, the tubes collapse due a limit moment instability which is followed by the formation of a kink on the compression flange of the tubes. The present research removes the limitation in the pre- bifurcation analysis and concentrates on the numerical prediction ANSYS -11 program of the response with stress and strain distribution on thin walled tubes of square cross section. The numerical, analytical and experimental results are converges to each other, by simulating the response of square tubes subjected to static and dynamic axial bending loading .The finite element models used for this work are featured by the geo-metric and material characteristics of square tubes and comparison of the computed bending response to the results and findings of the experimental works shows that the finite element models described here, approached the actual bending response of the square tubes to a satisfactory degree both in terms of collapse modes and main bending characteristics such as bending stress and strain and deformation displacement.
Keywords:- Finite element model, square shell, bending.

INTRODUCTION

Thin walled tubes are commonly used as structural members in many engineering application to resist axial and bending loads it was realized by researchers in the 1920 that the deformation of the cross section which accompanies bending could influence the response, strength and stability of such tubes , Hassan and Hancock [(1)] studied tubes with rectangular cross section and found that as bending proceeded, the bending moment of the tubes suddenly

dropped when a kink formed in the compression flange. Corona[2] and Vaze [3] presented an experimental investigation of circular and cylindrical cross section under bending with emphasis on the elastic-plastic case. The compressive properties and response of square tubes subjected to static axial and compression impact are investigated by means of numerical simulation using the LS-DYNA3D explicit finite element cod. Simulation works focused on modeling the three modes of collapse (i.e. bending, local tube wall buckling and mid-length unstable crushing) that were observed during the experimental works in reference[2] .The present numerical work aims to contribute to the analysis and investigation of the bending characteristics by simulating the response of square tubes subjected to static loading, using (ANSYS -11) finite element program.

The results of bending operation are affected by the plate, the tools and procedure employed for typical tensile strength values ,so the stronger and harder the plate ,the higher the necessary bending force, the great will be the spring back ,the larger the punch radius needed, the greater the necessary die opening width. considering plate thickness (t) as a general rule, thinner plate can be bent to smaller radii at right angels, the right punch radius is the most important factor, the bending angle, if the bent angle is smaller a punch with a smaller radius that has a lesser effect on the force needed and the spring back than the die width, spring back can be compensated by over bending by the same number of degrees.

ANALYTICAL MODEL

The formulation considers a tube with rectangular cross section of length (2L) the tubes develops a bending moment (M) upon being bent to curvature (R=1/K) as shown in fig.(1-a)the cross section has wall thickness (t) flange width (b) and web height (h) as shown in fig.(1-b) to accommodate slight variations from the nominally square cross section of the tubes as observed in the experiments . The curvature is assumed to remain constant along the tube. further more, deformations are assumed to be symmetric about plane (A-A) in fig. (1-a) and the plane of bending, the domain consists of the three regions shown in fig.(1-b) half of the upper flange and web and half of the lower flange which are denoted (1) ,(2) and (3) respectively. The coordinates used are also shown in fig.(1-b). The coordinates along the tube axis is denoted by(s) the (y_i)coordinate run a long the mid surface of each region and the z_i coordinates point in the respective through –thickness directions ,the common assumption that plane sections originally perpendicular to the (s) and (y_i) axes remain plane during loading is adopted for all three region .

The kinematics employed are based on thin shell theory, in order to derive the strain – displacement relation ship, employ the deformation composition scheme which is based on the work of Fabian O.[(5)]. For square tubes under bending, the objective of the scheme is to derive the expressions for the strain in a deformed tube and the displacement components in each region are shown in fig. (1). the first and second fundamental form for the imperfect straight tube ($a^{0(i)}$) and ($b^{0(i)}$) can be found from the respective form of a perfect straight tube as following. The total strain increment is assumed to be given by the sum of elastic and plastic components, the elastic components { $d\varepsilon^e_{ss}$, $d\varepsilon^e_{yy}$, $d\gamma^e_{sy}$ } are related to the stress increment ($d\sigma_{ss}$, $d\sigma_{yy}$, $d\tau_{sy}$) through[(6)(7)].

$$\begin{bmatrix} d\varepsilon^e{}_{ss} \\ d\varepsilon^e{}_{yy} \\ d\gamma^e{}_{sy} \end{bmatrix} = \frac{1}{E}\begin{bmatrix} 1 & -\nu & 0 \\ -\nu & 1 & 0 \\ 0 & 0 & 2(1+\nu) \end{bmatrix}\begin{bmatrix} d\sigma_{ss} \\ d\sigma_{yy} \\ d\tau_{sy} \end{bmatrix} \quad \ldots\ldots\ldots\ldots\ldots\ldots (1)$$

Where E is Young's modulus and ν is Poisson's ratio. the plastic strain components are given by:

$$\begin{bmatrix} d\varepsilon^p{}_{ss} \\ d\varepsilon^p{}_{yy} \\ d\gamma^p{}_{sy} \end{bmatrix} = \frac{9}{4\sigma_e^{\,2}}\left(\frac{1}{E_t}-\frac{1}{E}\right)\times\begin{bmatrix} S_{ss}S_{ss} & S_{ss}S_{yy} & 2S_{ss}S_{sy} \\ S_{yy}S_{ss} & S_{yy}S_{yy} & 2S_{yy}S_{sy} \\ 2S_{sy}S_{ss} & 2S_{sy}S_{yy} & 4S_{sy}S_{sy} \end{bmatrix}\begin{bmatrix} d\sigma_{ss} \\ d\sigma_{yy} \\ d\tau_{sy} \end{bmatrix} \quad \ldots\ldots\ldots\ldots (2)$$

Where S_{ss} ,S_{yy} and S_{sy} are components of the deviatoric stress and σ_e is the equivalent stress given by:

$$\sigma_e = \sqrt{\sigma^2{}_{ss} - \sigma_{ss}\sigma_{yy} + \sigma^2{}_{yy} + 3\tau^2{}_{sy}} \quad \ldots\ldots\ldots\ldots (3)$$

$$\varepsilon = \frac{\sigma}{E}\left[1+\frac{3}{7}\left(\frac{\sigma}{\sigma y}\right)^{n-1}\right] \quad \ldots\ldots\ldots\ldots (4)$$

The initial yield surface is given by

$\sigma_e - \sigma_0 = 0$

where σ_0 is the stress at the proportional limit of the uniaxial stress-strain curve .subsequent yield surfaces are given by:

$\sigma_e - \sigma_{emax} = 0$…………………………………………………………..…..….(5)

where σ_{emax} represents the largest equivalent stress achieved during the loading history. the displacement components u_i ,v_i and w_i are discredited using the trigonometric series listed in appendix A

The external work (w) required bending a unit length of tube up to a curvature r was then determined by integrating the moment – curvature response,

$$W = \int_{0}^{KL} M d_k \quad \ldots\ldots (6)$$

$$\frac{w}{h} = \{1+\cos(\frac{2\pi y_1}{b_o})\}[\frac{a\Delta}{2}\mathrm{Cos}(\frac{2\pi s}{\lambda})+\frac{b\Delta}{2}\mathrm{Cos}(\frac{2\pi s}{7\lambda})] \quad \ldots\ldots (7).$$

Where a_Δ measurements of the decrease in height of the cross section in the plane of bending. b_o is the second fundamental forms for the imperfect straight tube

Experimental results based on pure bending of a steel 4130 seamless square tube with h/t varied according to the change in shell tube thickness as =28.6 ,20.4 and 15.4 The nominal height of the cross section was h=25.4 ,25.52 and 25.29 mm and the length of the specimen was 0.76m . Shell thicknesses were 0.886, 1.21 and 1.61 mm. The experimental set – up and procedure are described in detail by Corona Ref[2] and [8] since agreed with it . The moment and curvature have been non dimensioalized by[9]:-

$M_o = 3/2\ \sigma_o t h^2$ and $k_1=3/2(\pi^2 t^2/(h^3(1-\nu^2)))$ ……..(8)

Where $\sigma_o = 0.2\ \sigma_y$ MPa and ν = Poisson ratio, the response was initially linear but become nonlinear as the material yielded. The bending process was stopped at predetermined values of curvature to make the measurements presented. Table 1 shows the chemical Composition of Medium Carbon Low Alloy Steel 4130 which is used in the study [10]. Better results obtained at the height to thickness ration were 20.49 since experimental results agreed with theoretical results and when compared with numerical result obtained from simulation process the three methods shows the same trend in all data under study (M,K and K_1).

NUMERICAL ANALYSIS

The first step in the finite element investigation was to develop the three models that simulated the experimental tests described in reference[2]. A detailed description of the modeled static and dynamic tests together with extensive analysis of the experimental results can be found in the referenced works [2]. The basic geometric and material data pertaining to the square tubes that were used in the three models described herein are listed in tabulated form in table .2 . The simulation process comes basely in three steps, first building the model according to the work-piece dimension and experimental environments included this

case, second loading the model to reach a curvature proportional to that of experimental results and third reading and recording the results. A model was built and data as in Table .2 was entered as shown in Fig. (2), the element type (shell 63) was chosen since it has both bending and membrane capabilities. Both in-plane and normal loads are permitted. The element has six degrees of freedom at each node: translations in the nodal x, y, and z directions and rotations about the nodal x, y, and z-axes.

Stress stiffening and large deflection capabilities are included. Real constant set -1 changed due to change in shell thickness value. Applying the material properties according to given data in table .2 that follow was the most important step before meshing the model to enable the program to apply the equation of finite element which the program built based on it Fig.(3).

Loading process occurred by applying bending moment in many steps to record the variation in height and the curvature dimensions due to applying and removing the load(bending moment) on the surface of the tube while keeping the ends constrained by applying a zero to displacement in all direction Fig.(4). K_1 was obtained from equation-8 with various σ_y taken from numerical ANSYS-11 results .The same procedure was applied non-dimensionalized the bending moment for each load step by M_0 calculated from equation -8 . Von -misses stress reading for each load step was recorded in additional to stress in y-direction used to obtain the value of k in equation -8. Von misses strain and stress recorded in each load step to have a total view of shells behavior due to bending process.

RESULTS AND DISSCUSSION

The results presented in this study were obtained by introducing a geometric imperfection in the initial configuration of the tube. The bending process was then simulated until a limit moment curvature was exceeded. The general response and stability characteristics of a given tube were deduced from the observed responses for various different types of initial imperfection .Ref.([2]) demonstrated that accurate prediction of the limit moment instabilities which lead to collapse , in the case of square tubes with sufficiently high h/t also may require a model which can take the development and growth of ripples into account .predictions obtained by neglecting the development of ripples yielded limit moments which were entirely due to uniform deformation of the cross section along the specimen .the difference between experimentally measured and ANSYS predicted limit moment curvature ranged from 8.7 percent for tubes with h/t =15.4 to 18.7 percent for tubes with h/t =28.6 .

Fig.(5) Shows the response of square tube upon being bent to a curvature in loading process, the max elastic plastic strain equivalent equal 0.462E-06 m in the end of tube and min strain 0.243 E-07 m, the ripples yield area in the middle surface of the tube . Fig.(6) shows the stresses equivalent in loading process when the max value equal 94753 Pa and min 4891 Pa. In Fig.(7) Response during stresses in y – direction with max and min value equal to 71284Pa, -58124 Pa. Fig. (8) shows the bending moment in x- direction with max value 168756 N.m, min value -168765 N.m .and the buckling in the ends of tube. Figure (9) shows strain distribution when elastic – plastic equal. max value 0.468E-06 m , min 0.1478 E- 7 . Fig.10 show the bending moment in Z- direction when max value 172249 N.m , min -172249 KN.m and the ripples yield area appear in the middle top surface of the tube section. Fig. (11) Show the last step bending stress in y- direction with max value 12149 N.m min -12831 N.m. Final response of square tube upon bent to a curvature R. Fig. (12) shows the elastic plastic equivalent strain with max value 0.256E-04 m , min 0.222E-7 m , final step bending response . Fig.(13) shows the stresses distribution due to unloading process after being bent to a curvature R with ratio 20.4. Fig.(14) show the bending moment in y-direction when max value 22836 N.m and min value -22836 N.m .

The theoretical response of M/Mo for the three models is shown in Fig. (15, 16, 17). Better results obviously obtained from Fig.(15) that bending moment equalized moment obtained from equation-8.Fig.(17) shows that for a tube with h/t = 28.6 , the reduction in k with increasing a_{Δ} is more drastic than for h/t= 20.4 at k/k1 = 5.40 . Compared to the uniform component than in the case with h/t=20.4 as shown in Fig.(16), in the fact the growth of the cross sectional Parameter Δ reverses at points close to s= (landa) $\lambda/2$,(where λ was chosen to be λ_{cr}=1.12 h which is the axial of the bifurcation mode calculated in Corona[2] and Vaze[3,4] on the other hand the reduction in k for increasing values of a_{Δ} is mild for tubes with h/t = 15.4 as shown in Fig. (17). Compares prediction of the growth of Δ which equal to the change in height y in ANSYS program at s = (landa) $\lambda/2$ with experimental measurements , the measurement device with respect to the ripples is unknown that is , it can not be correlated to a specific value of s , it can be expected however that the predicted responses will bound the experimental measurements , the differences between experiment and analysis is (0.01,0.125,0.16,6)percent for Figs (15,16,17,18) respectively, in all cases , the somewhat abrupt change in the curvature of experimental curves in Fig.(18) , measurement of the decrease in height of the cross section in the plane of bending (denoted by Δ) as a function of axial position for several values of curvature is shown in Fig.(19 , 20) .

a little estimation shows that as the height to thickness ratio decreased to 20.49 stress concentration on constraint location describing rigid motion abilities was decreased causing the deformation of the tube due to stress concentration to be less and the local buckling caused due to forming of a ripple along the axial length to be less and less which lead to more stability and high response of the tube. Fig. (21) shows Response of tube h/t = 28.6, h/t =20.4, h/t= 15.4 Comparison of the measured sensitivity of the moment curvature with K/K1.

CONCLUSIONS

In this study the results obtained agreed well(as mentioned above) with experimental data and suggest that collapse of the tubes is imperfection sensitive, the degree of imperfection sensitivity is Particularly high for tubes in the high end of the range of h/t > 18, from observation of the experimental result . while collapse of tubes with low h/t is relatively imperfection insensitive , in fact in case with h/t = 15.4 , the axial variation in cross section deformation is not very significant in the determination of the limit moment curvature and can be neglected . The tube used in the experiment had long wavelength imperfection components of amplitude five times larger than that of components with wavelengths in the order of that of the buckling mode.

The results obtained here however indicate that the effect of such long wavelength component in the imperfection can be neglected in calculation of limit moment curvature. The phenomenon of ripple localization and formation of the kink which appears on the compression flange of the tubes upon collapse was successfully simulated by introducing an imperfection in which the amplitude of the ripples is biased. Again , The comparison was very good. The present study, which includes the curvature into account, seems to give accurate results compared to experiments(which is more accurate) and theoretical predictions. However, it still overestimates the ultimate moment, especially for high h/t tubes. This can be explained that, for tubes with high h/t ratios, the plasticity does not spread linearly along the whole length as it is assumed in the analysis. In contrast, the plasticity tends to concentrate at the plastic hinge region and causes premature failure.

REFERENCES

1. Hassan, S.w. And Hancock .G.J., 1989 "Plastic Bending Test of Cold Formed Rectangular Hollow Section" Journal of the Australian Institute of Steel Construction Vol. 23, pp. (2-19).

2. Corona .E. and Vaze, S.P, 1996, "Buckling of Elastic – Plastic Rectangular Tubes and Bending" International Journal of Mechanical Sciences, Vol.38, PP. (753-775)
3. Kyriakides S. and J.U.GT , 1992,"Bifurcation and Localization Instabilities in Cylindrical Shells under Bending Part (1)" ,Experiments International Journal of Solids and Structures, Vol. 29 PP (1117 – 1142) .
4. J.U.GT and Kyriakides1992, "Bifurcation and Localization Instabilities in Cylindrical Shells under Bending Part (2) ,Experiments International Journal of Solids and Structures, Vol. 29, PP (1134– 1171).
5. Fabian. O. 1981 "Elastic – Plastic Collapse of Long Tubes Under Combined Bending and Pressure Load", Ocean Engineering Vol. 8 ,PP (295 – 330) .
6. Sanders J.1,1993 "Nonlinear, Theories for Thin Shells " Quarterly of Applied Mathematics Vol. 21, PP. (21-36) .
7. John Bird, 2006, "Higher Engineering Mathematic" Fifth Edition ,PP (705- 737).
8. Saad .Th. F, 2007 " Estimating the Effect of Spring back Due to Bending Process of Semi Conical Shells " Diyala Journal of engineering science, Vol. 3, No 2, PP.(65- 75) .
9. S.J. HU, 2002, "Mechanics of Sheet Metal Forming" Second Edition, the University of Michigan , USA Publish by Butterworth- Heinemann , PP (92 -101) .
10. E.J. Hearn, 1988,"Mechanics of Materials 2nd Edition" International Series of Materials Science and Technology Vol. 19 , Pp (429)
11. F.C. Campbell,2006, "Manufacturing Technology for Aerospace Structural Materials" Elsevier Ltd, the Netherlands U.S.A , PP 187 .

Appendix A

The displacement components u_i ,v_i and w_i are discredited using the trigonometric series listed as:-

$$u_1 = \varepsilon_{ss} s + \sum_{m=1}^{n} (a_{0m} + \Sigma\, a_m \cos(\frac{l\pi y}{bo})) \sin(mps). \quad \text{---------- (9)}$$

$$v_1 = \sum_{m=0}^{n} (a_{0m} y_1 + \sum_{l=1}^{nf} a_m \sin(\frac{l\pi y}{bo})) \cos(mps) \quad \text{---------- (10)}$$

$$w_1 = \sum_{m=0}^{n} (a_{0m} + \sum_{l=1}^{nf} a_m \cos(\frac{l\pi y}{bo}) \cos(mps) \quad \text{---------- (11)}$$

$$u_2 = \varepsilon_{ss} s + \sum_{m=1}^{n} (b_{0m} + \Sigma\, [\, b_m \cos(\frac{l\pi y}{bo}) + c_m \sin(\frac{l\pi y}{bo}) \quad \text{---------- (12)}$$

$$v_2 = \sum_{m=0}^{n} (b_{0m} + c_{om} y_2^2 + \sum_{l=1}^{nf} [b_m \cos(\frac{l\pi y}{bo}) + c_m \sin(\frac{l\pi y}{bo})]) \cos(mps) \quad \text{--------(13)}$$

$$w_2 = \sum_{m=0}^{n} (b_{0m} + \sum_{l=1}^{nf} a_m \cos(\frac{l\pi y}{bo}) + c_m \sin(\frac{l\pi y}{bo})]) \cos(mps) \quad \text{---------- (14)}$$

$$u_3 = \varepsilon_{ss} s + \sum_{m=1}^{n} (d_{0m} + \Sigma d_m \cos(\frac{l\pi y}{bo})) + \sin(\frac{l\pi y}{bo}) \quad \text{---------- (15)}$$

$$v_3 = \sum_{m=0}^{n} (d_{0m} y_3 + \sum_{l=1}^{nf} [d_m \sin(\frac{l\pi y}{bo}) \cos(mps) \quad \text{---------- (16)}$$

$$w_3 = \sum_{m=0}^{n} (d_{0m} \sum_{l=1}^{nf} d_{im} \cos(\frac{l\pi y}{bo})) \cos(mps) \quad \text{---------- (17)}$$

where a ,b ,d ,m ,n and I are region for the tube cross section used in trigonometric series,p=π/L

Sanders' Kinematics

$$E_{ss}^{(i)} = \frac{u_{i.s}}{\alpha_s^{(i)}} + \frac{\alpha_{s.y}^{(i)} v_i}{\alpha_s^{(i)} \alpha_{yi}^{(i)}} + \frac{w_i}{R_s^{(i)}} + \frac{1}{2}\phi_s^{(i)^2} + \frac{1}{2}\phi^{(i)^2} \quad \text{..... ..... (A1)}$$

$$E_{y_i y_i}^{(i)} = \frac{u_{i.y_i}}{\alpha_{y_i}^{(i)}} + \frac{\alpha_{y_i.s}^{(i)} u_i}{\alpha_s^{(i)} \alpha_{yi}^{(i)}} + \frac{w_i}{R_{y_i}^{(i)}} + \frac{1}{2}\phi_{y_i}^{(i)^2} + \frac{1}{2}\phi^{(i)^2} \quad \text{..... .....(A2)}$$

$$E_{sy_i}^{(i)} = \frac{1}{2}\left[\frac{v_{i.s}}{\alpha_s^{(i)}} + \frac{u_{i.y_i}}{\alpha_{y_i}^{(i)}} - \frac{\alpha_{s.y_i}^{(i)} u_i}{\alpha_s^{(i)} \alpha_{yi}^{(i)}} - \frac{\alpha_{y_i.s}^{(i)} v_i}{\alpha_s^{(i)} \alpha_{yi}^{(i)}} + \phi_s^{(i)} \phi_{y_i}^{(i)}\right] = E_{y_i.s}^{(i)} \quad \text{..... ....(A3)}$$

$$K_{ss}^{(i)} = \frac{\phi_{s.s}^{(i)}}{\alpha_s^{(i)}} + \frac{\alpha_{s.y_i}^{(i)} \phi_{y_i}^{(i)}}{\alpha_s^{(i)} \alpha_{y_i}^{(i)}} \quad \text{..... .... (A4)}$$

$$K_{y_i y_i}^{(i)} = \frac{\phi_{y_i.y_i}^{(i)}}{\alpha_{y_i}^{(i)}} + \frac{\alpha_{y_i.s}^{(i)} \phi_s^{(i)}}{\alpha_s^{(i)} \alpha_{y_i}^{(i)}} \quad \text{..... ....(A5)}$$

$$K_{s.y_i}^{(i)} = \frac{1}{2}\left[\frac{\phi_{y_i.s}^{(i)}}{\alpha_{s_i}^{(i)}} + \frac{\phi_{s.y_i}^{(i)}}{\alpha_{y_i}^{(i)}} - \frac{\alpha_{s.y_i}^{(i)} \phi_s^{(i)}}{\alpha_s^{(i)} \alpha_{y_i}^{(i)}} - \frac{\alpha_{y_i.s}^{(i)} \phi_{y_i}^{(i)}}{\alpha_s^{(i)} \alpha_{y_i}^{(i)}} + \left(\frac{1}{R_{y_i}^{(i)}} - \frac{1}{R_s^{(i)}}\right)\phi^{(i)}\right] = K_{s.y_i}^{(i)} \quad \text{.....(A6)}$$

Where :

$$\phi_s^{(i)} = \frac{-w_{i.s}}{\alpha_s^{(i)}} + \frac{u_i}{R_s^{(i)}} \quad \text{..... ....(A7)}$$

$$\phi_{y_i}^{(i)} = \frac{-w_{i.y_i}}{\alpha_{y_i}^{(i)}} + \frac{v_i}{R_{y_i}^{(i)}} \quad \text{..... ....(A8)}$$

And , for a toroid of rectangular cross section.

$\alpha_s^{(1)} = 1 - h_0 k/2$ $\quad \alpha_{y_1}^{(1)} = 1$ $\quad 1/R_s^{(1)} = -1/(1/k - h_0/2)$ $\quad 1/R_{y_1}^{(1)} = 0$

$\alpha_s^{(2)} = 1 + k y_2$ $\quad \alpha_{y_2}^{(2)} = 1$ $\quad 1/R_s^{(2)} = 0$ $\quad 1/R_{y_2}^{(2)} = 0$

$\alpha_s^{(3)} = 1 + h_0 k/2$ $\quad \alpha_{y_3}^{(3)} = 1$ $\quad 1/R_s^{(3)} = -1/(1/k + h_0/2)$ $\quad 1/R_{y_3}^{(3)} = 0$

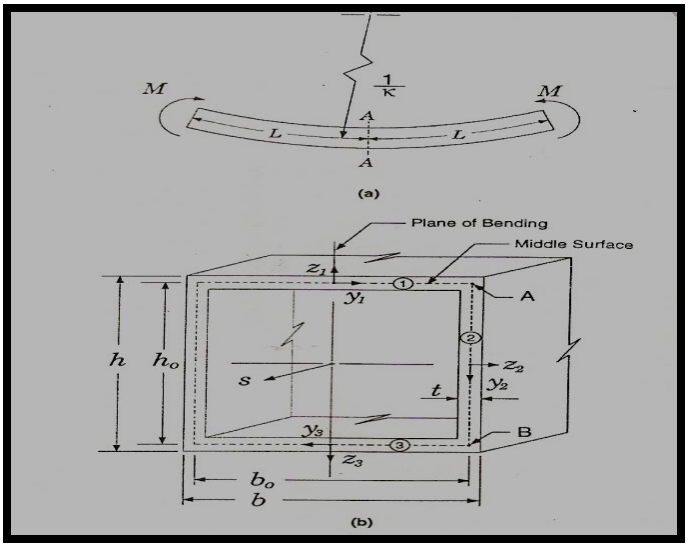

Fig.(1): Model of Shell Square Tubes Used in Theoretical Study.

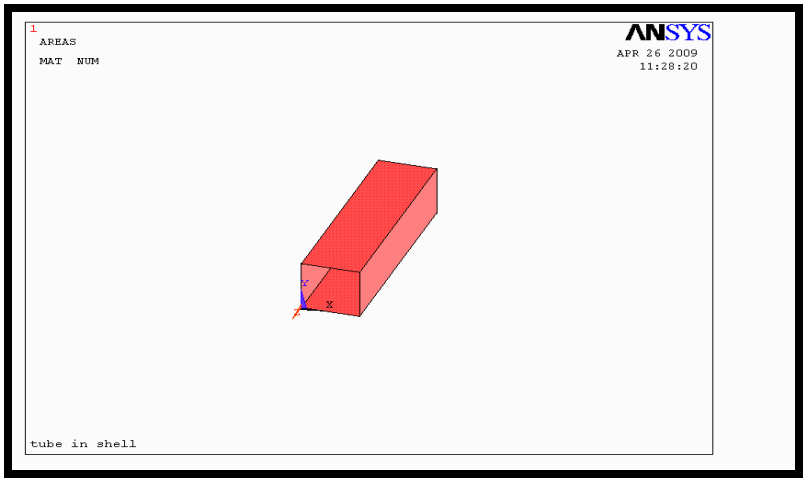

Fig. (2): Numerical Model of Square Shell Tubes Used in Study by ANSYS-11.

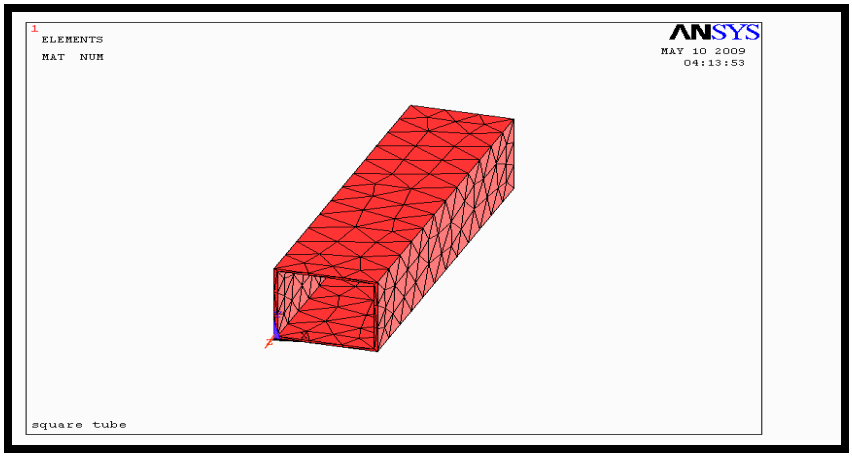

Fig. (3): ANSYS (11) Mesh Forming used in the Study.

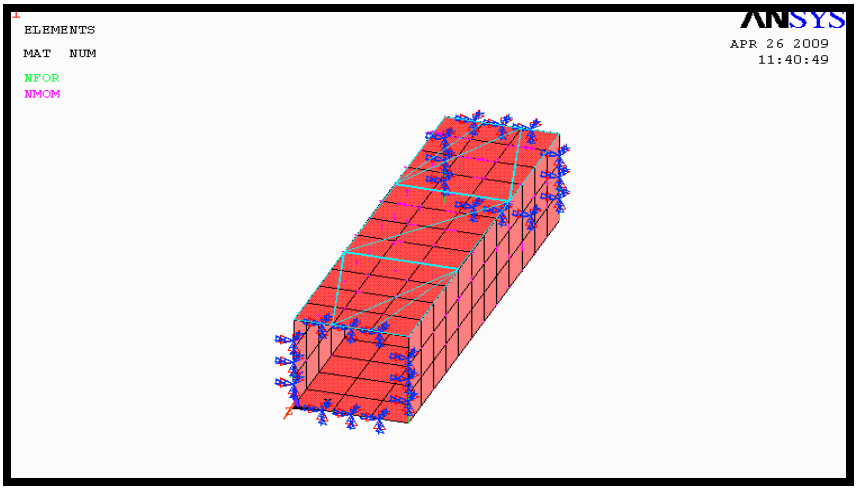

Fig.(4): Numerical Loading Process used in the Study.

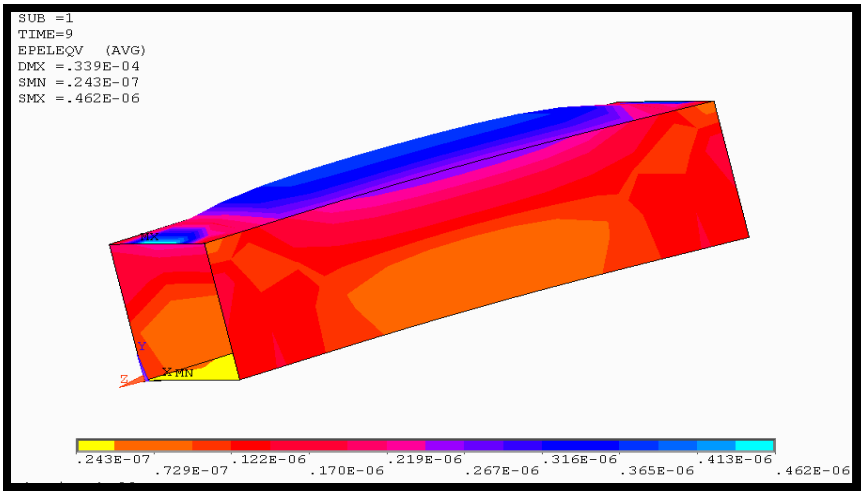

Fig. (5): Response of Square Tube upon Being Bent to a Curvature R and Show Strains in Loading Process.

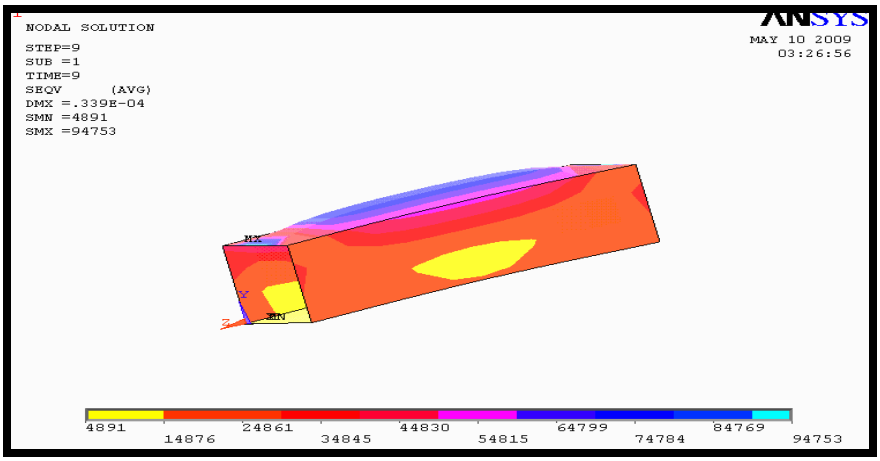

Fig.(6): Response of Square Tube upon Being Bent to a Curvature R and Show Stresses in Loading Process.

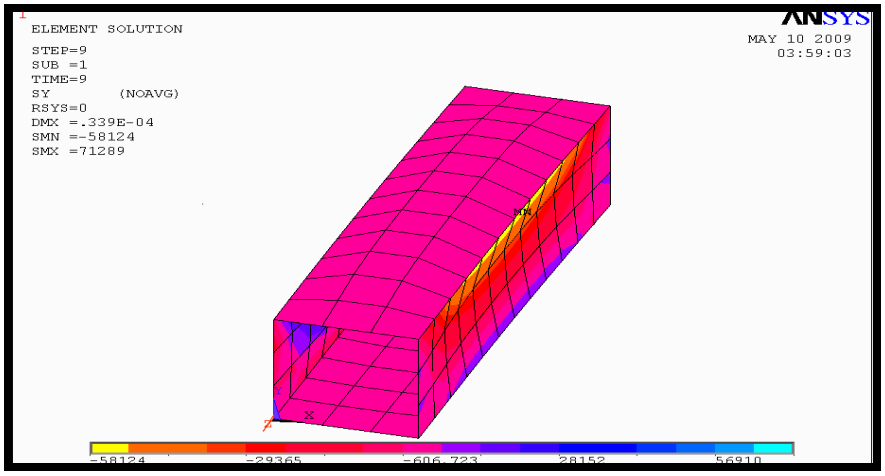

Fig.(7): Response of Square Tube upon Being Bent to a Curvature R and Show Stresses in Y Direction .

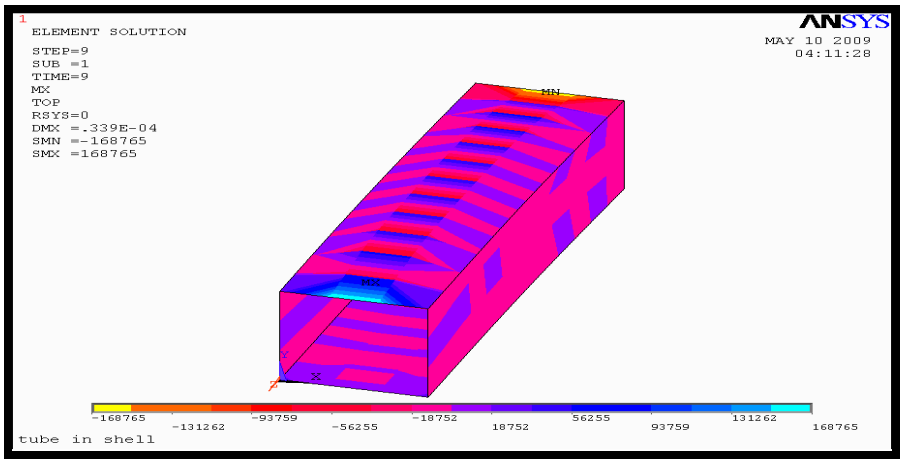

Fig. (8): Shows the bending moment in x- direction and the buckling in the ends of tube.

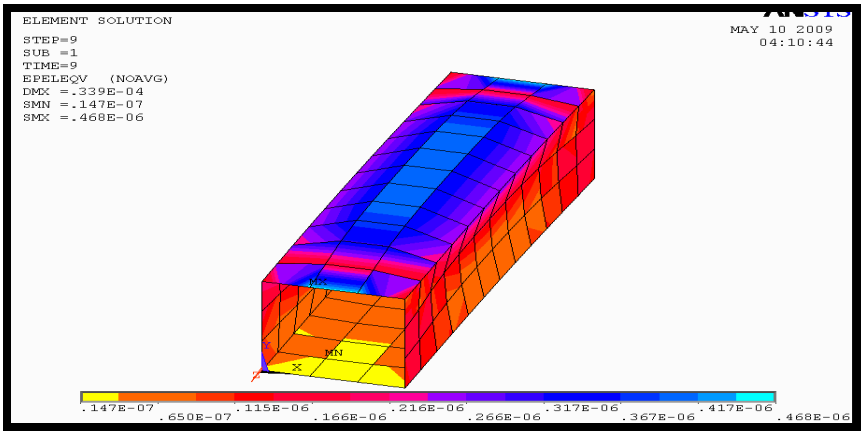

Fig.(9): shows strain distribution on tube sides at elastic – plastic bending.

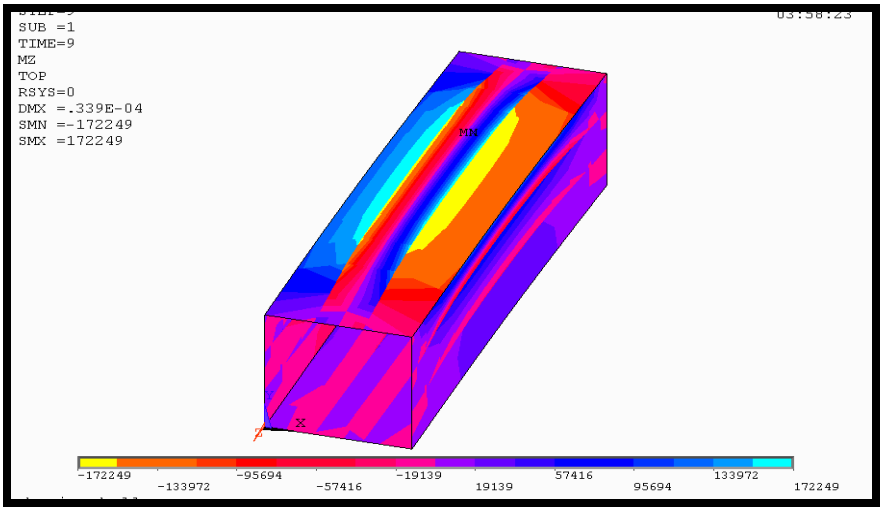

Fig. (10): Bending Moment in Z – Direction.

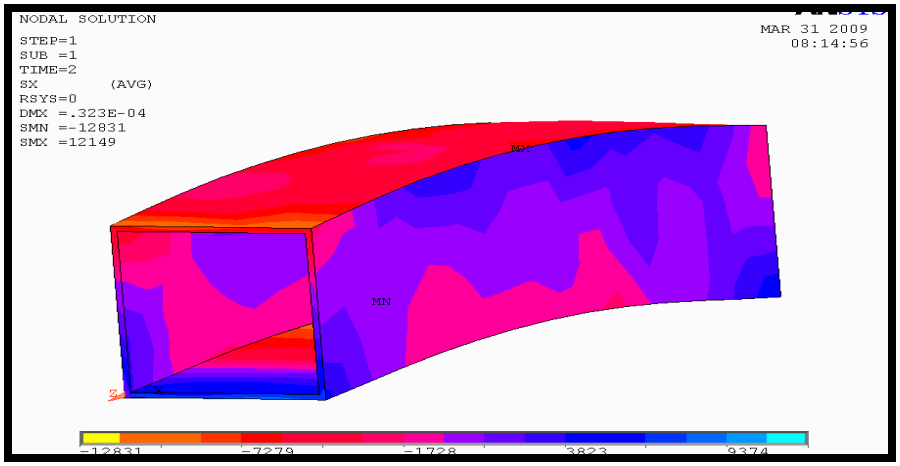

Fig.(11): Last bending Stress in y direction.

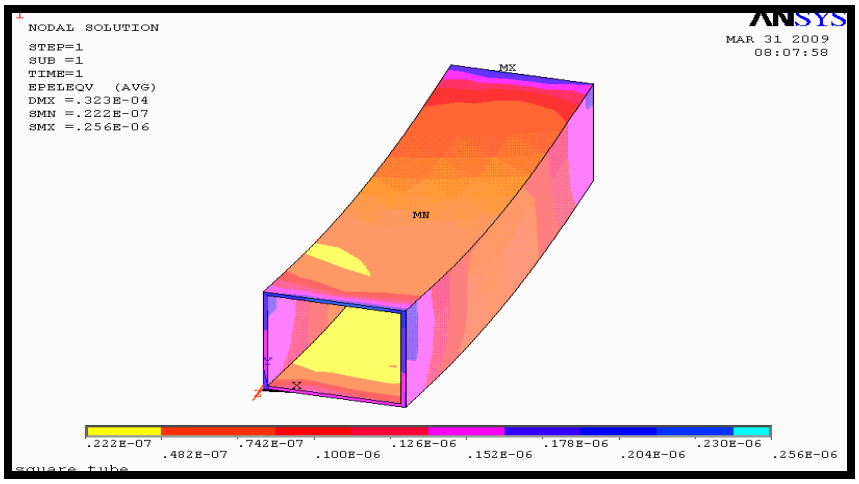

Fig.(12): Final Response of Square Tube upon Being Bent to a Curvature R.

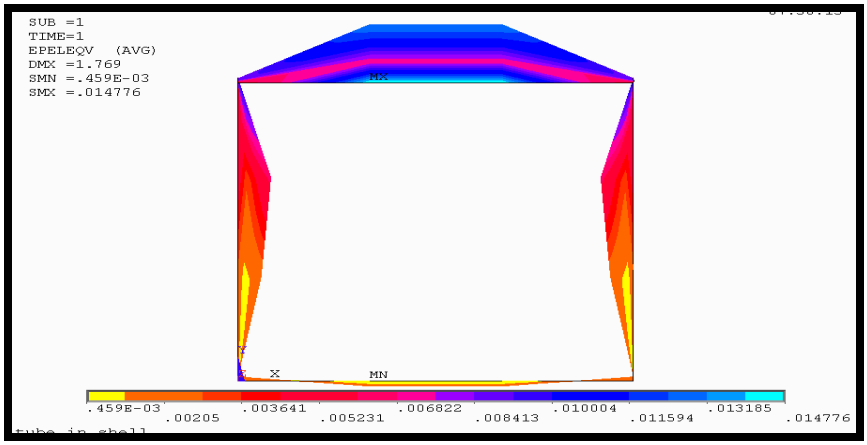

Fig.(13): Stress Distribution due to Loading and unloading Process in Third step of Loading Procedure.

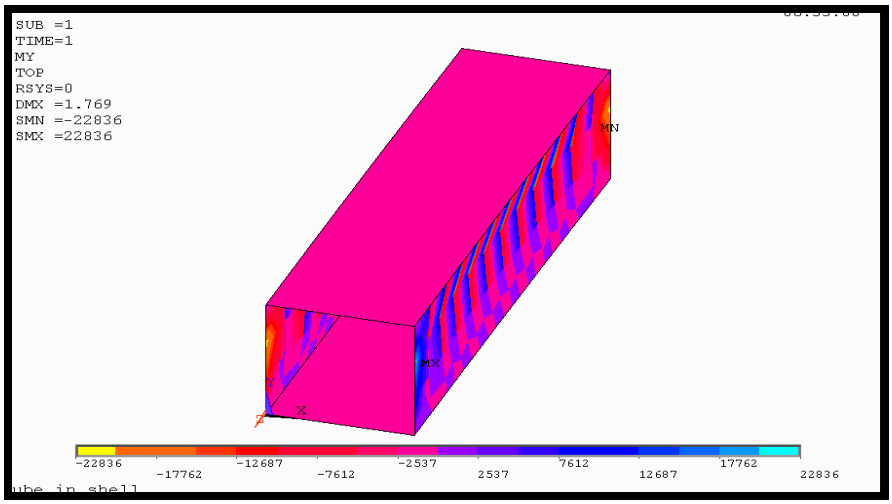

Fig. (14): Bending Moment in Y direction when it loaded in the last step.

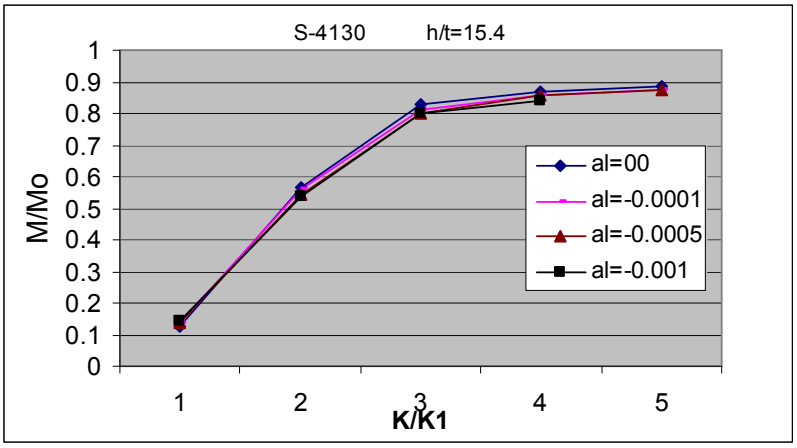

Fig. (15): Response of a tube with h / t = 15,4 Sensitivity of the moment Curvature Response to the Severity of Initial ImperfectionW.

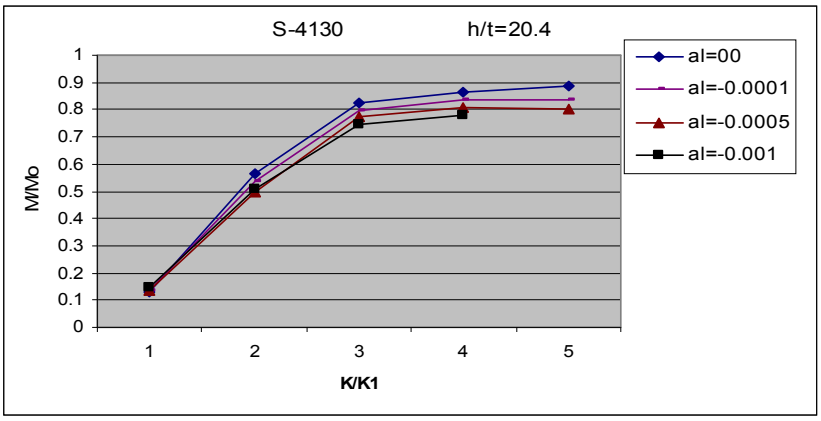

Fig. (16): Response of a tube with h / t = 20.4 Sensitivity of the moment Curvature Response to the Severty of Initial Imperfection ω.

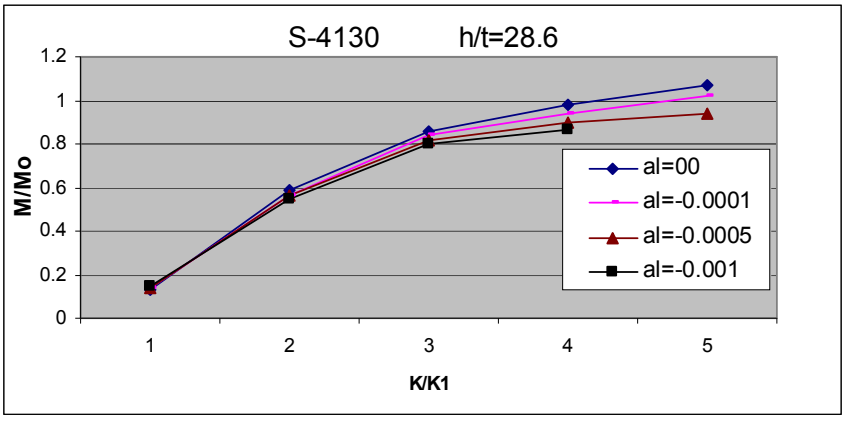

Fig. (17): Response of a tube with h / t = 28.6 Sensitivity of the moment Curvature Response to the Severity of initial Imperfection ω.

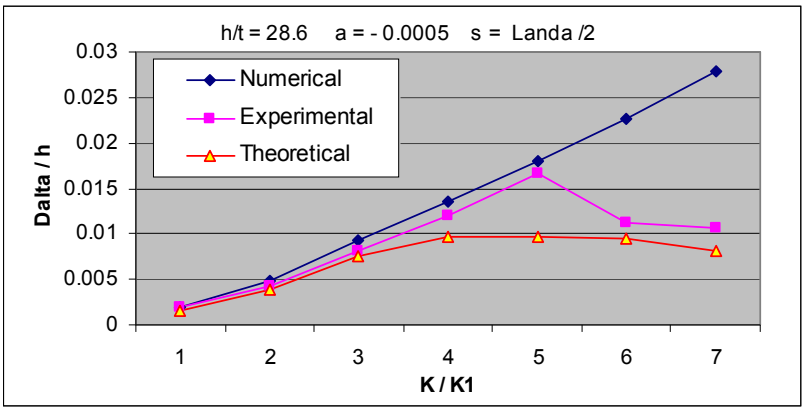

Fig. (18): ComParison of Experimental and Theoretical Result with Numerical Prediction in the Measured Growth of Dalta(Δ) for h / t = 28.6.

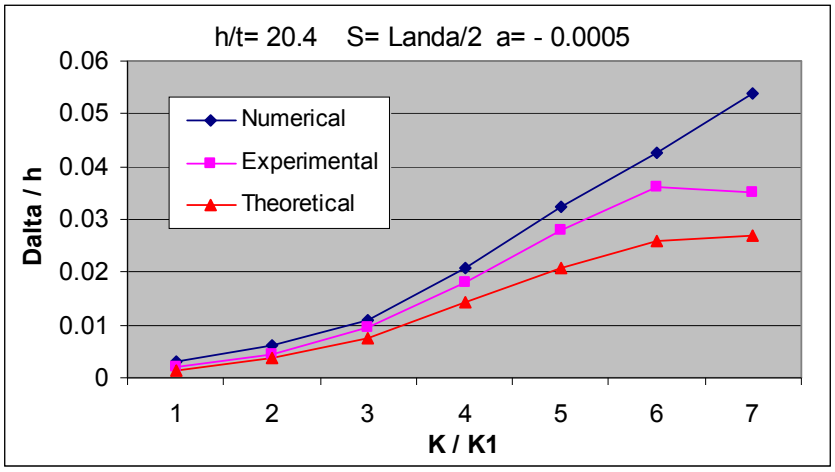

Fig. (19): ComParison of the Measured Growth of Dalta(Δ) in, Experimental and theoretical with the Prediction in Numerical Result for h / t = 20.4.

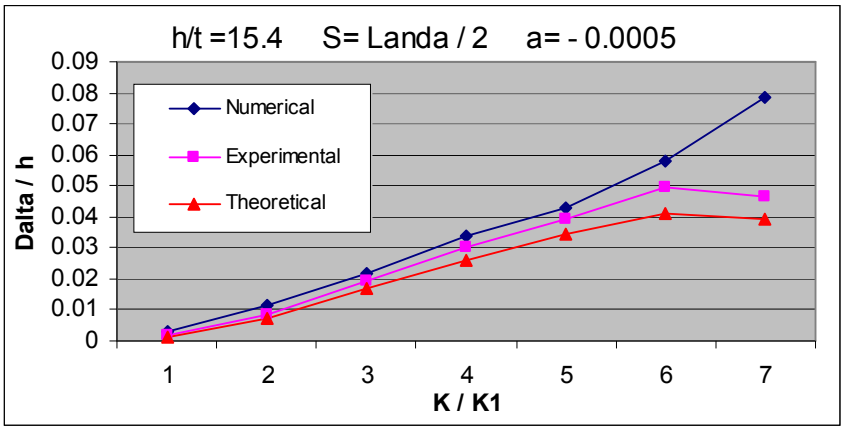

Fig. (20): ComParison of the Measured Growth of Dalta(Δ) in Experimental and Theoretical Result with Numerical Prediction for h / t = 15.4.

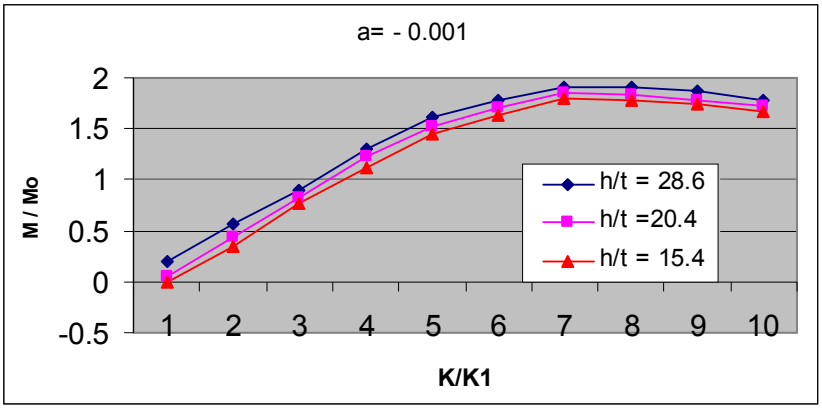

Fig. (21): Comparison of the Measured Sensitivity of the Moment Curvature with K/K1 Response of tube h/t = 28.6, h/t =20.4,h/t= 15.4.

التحليل المرن –اللدن للانابيب القشرية المربعة عند تعرضها للانحناء باستخدام العناصر المحددة

اخلاص عيدان قادر

مدرس مساعد

كلية الهندسة_ جامعة ديالى

الخلاصه

في هذه الدراسة تم ايجاد نموذج تحليلي لغرض الحصول على الخواص الغيرخطية الكينيماتيكية لمواكبة التطور في التطبيقات الهندسية ولغرض مقاومة الاجهاد الانحنائي لانابيب قشرية الجدران في الحالة المرنة واللدنة لاستعمالها في الهياكل الانشائية .اوضحت النتائج ان الانهيار في مثل هذه الانشاءات ناتج عن الحساسية لوجود الشوا ئب (ذات ارتفاع الى سمك معين) ‘حيث تقل الحساسية بنقصان هذه النسبة .عمليا تفشل الانابيب نتيجة عدم الاستقرار في حدود العزم والتي يتبعها تكون انبعاجات في الجانب الضغطي للانابيب. يزيل البحث الحالي التحديدات التي تعيق التحليل ويركز على التنبؤ العددي بواسطة برنامج حاسوبي (Ansys.11) لمعرفة الاستجابة مع توزيع الاجهادات والانفعالات.

اقترنت النتائج العملية والتحليلية والعددية مع بعضها عند مقارنة استجابة الانابيب المربعة الشكل ذات الجدران القشرية التي يسلط عليها احمال انحنائية مستقرة ومتغيرة ,ان النماذج التي طورت لهذا العمل اظهرت خواص المادة وتركيبها وعند المقارنة تبين ان النتائج العملية والنتائج المقروءة من (F.E.M.) تتقارب مع بعضها البعض بدرجة مقبولة جدا من حيث طور الانهيار وخواص الانحناء من اجهاد وانفعال ومقدار المسافة للتشوية .